Optical Characterization of Potential Dampening in Dendritic Spine Electrophysiology

Kim, Samuel[1], Sakamoto, Masayuki[2], and Yuste, Rafael[3]
[1]Columbia College, Columbia University, New York, NY 10027, USA
[2]Department of Biological Sciences, Columbia University, New York, NY 10027, USA
[3]Department of Biological Sciences, Kavli Institute for Brain Science, Columbia University, New York, NY 10027, USA

Abstract

This study aims to quantitatively characterize the electrophysiology of the dendritic spine as compared to that of its adjacent dendritic shaft, by imaging artificially induced back-propagating action potentials using a variety of different genetically encoded voltage indicators. We performed whole cell patch clamp and current injection recordings with simultaneous voltage imaging of neonatal mouse hippocampal neurons, which were transfected to express 'ArcLight' or one of two variants of 'Archaerhodopsin 3 (Arch)' known as 'QuasAr1' and 'QuasAr2'. With ArcLight, we coupled electrophysiological current injection recordings with fluorescence imaging and compared the individual peak fluorescence change ($\Delta F/F$) value of each spine with the peak $\Delta F/F$ value of its adjacent dendritic shaft in response to induced back-propagating action potentials. The results from ArcLight do not indicate a statistically significant dampening in membrane potential from the dendrite shaft across an adjacent spine, but do suggest a difference in membrane potential fluctuations between long pulse (100msec) and short pulse (20msec) current injections. With Arch, we quantified the $\Delta F/F$ values from current injection recordings and voltage imaging sessions of neuronal soma for 'QuasAr1' and 'QuasAr2'. Preliminary current injection and soma imaging results initially exhibited negligible signal-to-noise ratios of $\Delta F/F$ in response to induced action potentials, possibly due to technical maladjustments. A subsequent, more general characterization of Arch using voltage clamp and voltage step manipulations with QuasAr1 at different laser intensities indicates that QuasAr1 shows large changes in fluorescence at much weaker laser intensities (~10 mW) than was used for aforementioned current injection voltage imaging (~110 mW). We intend to further optimize and apply QuasAr1 and QuasAr2 to spine imaging, and subsequently investigate the difference in peak $\Delta F/F$ values for different current injection pulse durations as suggested by ArcLight imaging data.

I. INTRODUCTION

The prevailing view on consciousness speculatively characterizes the mind as 'emergent', meaning that it is unobserved on a microscopic level but emerges as a macroscopic property due to the collective interactions of its components, i.e., neurons. In order to understand the macroscopic workings of the brain, it inevitably follows that we must thoroughly decode the dynamic real-time communications that occur across the micro-circuitry between neurons[1]. Considering the extent of electrophysiological variation that is present even on the level of an individual neuron, however, it would be useful to first characterize the elusive small-scale electrophysiological components of neuron-to-neuron communication; one such component being the dynamics of membrane potential fluctuation in dendritic spines.

Dendritic spines are, as the name implies, small protoplasmic protrusions on the surface of the dendritic shaft of a neuron that are known to be postsynaptic contact points with the axons of presynaptic neurons[2]. Previous studies have proposed and tested a number of hypotheses on the function and utility of these structures, such as linear integration of electrical input and prevention of dendrite potential saturation[2, 3,4], biochemical compartmentalization and contribution to long term potentiation[5], and preservation of the rapid time course of action potentials (APs) in affecting synaptic

plasticity within a small time window[6]. In particular, we place interest in the suggested electro-physiological compartmentalization of spines in the course of a neuron's processing of multiple inputs; in other words, the function of some sort of alteration of membrane potentials that flow between the shaft of a dendrite and its adjacent spine.

The advent of techniques capable of direct measurement of potential on such a miniscule and rapid scale in dendritic spines, as opposed to indirect methods such as calcium imaging which utilizes delayed calcium dynamics as a proxy[7, 8], is relatively new. Voltage imaging, one of the particularly promising optical methods, utilizes voltage indicators, which usually consist of a complex of proteins that respond to fluctuations in electrical potential by undergoing a conformational change and altering their fluorescence emission. By embedding these indicators in the plasma membrane of a neuron, it is possible to make accurate measurements of membrane potential dynamics with fluorescence change as a proxy[9].

Of particular interest in this study are two distinct genetically encoded voltage indicators known generally as 'ArcLight' and 'Arch (Archaerhodopsin 3)'. ArcLight utilizes a complex between the voltage-sensitive domain of *Ciona Intestinalis'* voltage-sensitive phosphatase and a Super ecliptic pHluorin (a modified GFP), and has been shown to undergo ~1% to ~5% negative changes in fluorescence in response to individual action potentials in mammalian neurons[10]. Variants of Arch, on the other hand, are derived from a single-channel bacterial rhodopsin (in other words, a light-activated ion channel) of *Halorubrum sodomense*, and, while exhibiting negligible fluorescence at baseline, have been shown to undergo positive increases in fluorescence of much greater magnitudes (up to ~100%, depending on variant) per 100mV of membrane potential change under intense laser illumination[11,12]. Hence, for the purposes of this study we adopt ArcLight as well as two variants of Arch known as QuasAr1 and QuasAr2 as genetically encoded voltage indicators to closely track electrophysiological dynamics in individual neurons[13].

In examining spine electrophysiology, we primarily utilize artificially induced back propagating action potentials (bAPs) to elicit membrane potential fluctuations in dendritic spines. bAPs are known to be primarily passively diffusing changes in membrane potential that propagate in reverse of the conventional direction, from the axon hillock towards the dendritic tree, as a result of regular elicited action potentials[14]. Thus by utilizing ArcLight and variants of Arch to image the membrane potential fluctuations that occur from bAPs induced by a variety of current injections, we seek to quantify and test the electrical compartmentalization theory of dendritic spines. Specifically, we address the potentially specialized treatment of and differential response to distinct electrical stimuli, through differences in the possible dampening of membrane potential from dendritic shaft to spine.

II. MATERIALS AND METHODS

A. Hippocampal Neuron Plating and Culture

Using 70% EtOH and UV-sterilized stainless steel surgery tools, we euthanized neonatal mouse pups (P0-P1) via instantaneous decapitation and dissected hippocampi under a light microscope and stored them temporarily in a separate 15 ml falcon tube. All procedures following decapitation took place in a cold dissection solution, made from 160 mM Sodium Chloride, 5 mM Potassium Chloride, 1.1 mM Magnesium Sulfate, 2 mM Magnesium Chloride Hexahydrate, 5 mM Hepes, 5.6

mM Glucose, 0.001g Phenol Red and titrated to pH 7.4. Following dissection, isolated hippocampi were incubated at 37 ℃ for 20 min. on a shaker in a filtered dissociation solution consisting of L-cysteine, calcium chloride, ethylene-diaminetetraacetic acid (EDTA) and papain dissolved in dissection solution. The supernatant was subsequently removed and replaced with a filtered papain deactivation solution, which consisted of trypsin inhibitor and albumin dissolved in complete medium consisting of Minimum Essential Medium (MEM) w/o L-glutamine (Invitrogen #11095-072), HI-glucose MEM, Serum extender, 100x (200 mM) L-glutamine (Sigma # G7513), and Heat Inactivated FCS (Thermo Fisher Scientific HyClone Products #SH30070.02HI). This was immediately replaced with regular complete medium, the hippocampal tissue further dissociated into individual cells via glass pipettes, and the obtained cells counted on a hemocytometer before being plated onto individual coverslips coated with Poly-L-lysine in a 24-well plate (cell density 75K-120K per coverslip). Following incubation overnight, the culture medium was completely replaced with Neurobasal Medium (NBM), which contained additives of B-27 supplement, L- glutamine and Penicillin/Streptomycin Solution. The medium was changed partially once a week.

B. E. Coli Transformation and Plasmid Propagation

DH5-alpha *E. Coli* from Invitrogen (www.invitrogen.com) stored in -80 ℃ were thawed, distributed into aliquots, and, after addition of a voltage indicator-encoding plasmid, were heat shocked at 42 ℃ for 45 s, followed by a 2 min. incubation on ice. The transformed cells were subsequently incubated in a ~37 ℃ water bath for 45 min., centrifuged and plated on LB agar plates, and incubated overnight at 37 ℃. A single colony of the transformed *E. Coli* was grown in 5 ml LB broth with Ampicillin, and incubated at 37 ℃ on a shaker for 8 hours. We then added a 1 ml aliquot to a 300 ml LB- Ampicillin culture and incubated the cells overnight on a 37 ℃ shaker. The plasmid was isolated from incubated *E. Coli* cultures according to the 'Endotoxin-free plasmid DNA purification' user manual's 'NucleoBond Xtra Maxi EF' protocol by Machery-Nagel GmbH and Co. KG, also accessible at www.mn-net.com. The purified plasmid was stored at -20 ℃.

C. Plasmid Vector Transfection

Transfections were performed 3-5 days after neuron plating. A mixture of the DNA plasmid, calcium chloride, double-distilled water, and 2X HEPES buffered saline (HBS) was incubated at RT for 20 minutes (total 30 μL for each coverslip). The entirety of the NBM for each culture was transferred to a 15 ml falcon tube and stored in a 37 ℃ incubator, and replaced with MEM (www.invitrogen.com). Each coverslip was subsequently transfected and incubated at 37 ℃ for 45 minutes. Afterwards, the coverslips were washed three times with MEM, and the previously collected NBM was re-applied to the coverslips. Transfection was allowed to take place over about a 1-2 day period.

D. Electrophysiology: Patch Clamping and Voltage Imaging

Coverslips were taken from the incubator for patching starting 2-3 days post-transfection. The stage and coverslip were superfused at room temperature in oxygenated artificial cerebrospinal fluid (ACSF) solution heated to ~37 ℃, diluted from a 10x ACSF stock of 126 mM NaCl, 26 mM sodium hydrogen carbonate, 1.145 mM sodium dihydrogen phosphate, 10mM dextrose, and 3 mM KCl, with additives of 1 M magnesium sulfate and 1 M calcium chloride. Micropipettes (Sutter Instruments:

Borosilicate glass capillaries) were pulled using a DMZ-Universal Puller (Zeitz-Instruments) to 4-7MΩ resistance, and filled with an internal pipette solution of 140 mM K-gluconate, 5 mM KCl, 0.2 mM EGTA, 2 mM $MgCl_2$, 2 mM Na_2ATP, and 10 mM HEPES, subsequently adjusted to pH 7.3 with KOH.

Hippocampal neurons were whole-cell patch clamped using a bright-field/epifluorescence microscopy setup equipped with a Mercury ArcLamp [For ArcLight (GFP): Excitation filter 480/40 (460-500) nm, DM 495 nm, Emission filter 535/550 nm. For Arch (mOrange reporter): Excitation filter 540/20 (530-550) nm, DM 570nm, Barrier filter 590 nm. For Arch (QuasAr1 and QuasAr2): Emission filter 700/75) and a x40 (N.A. 0.8) or x60 (N.A. 0.9) objective setup mounted with an EMCCD camera (Product: ImageEM (Hamamatsu)) and four pipette manipulators. Whole-cell patch clamping was performed using Axon Multiclamp 700B amplifiers (Molecular Devices), digitized at 10 kHz with National Instruments 6259 multichannel cards and recorded using custom software written using LabView (National Instruments). We used the Multiclamp and PackIO softwares to hold voltage at -65 mV and apply and record current/voltage. For ArcLight, we performed current injection protocols, each protocol injecting 250 pA pulses for 10 times at regular intervals over a period of ~12 seconds, each pulse lasting 20 ms (short) or 100 ms (long). The PackIO recordings were coupled with fluorescent voltage imaging recordings that were performed under 570nm excitation. For Arch, we initially also performed current injection protocols, each protocol injecting 250 pA pulses for 30 times at regular intervals over a period of ~33 seconds, each pulse lasting 20 ms (short) or 200 ms (long). In addition, for Arch we performed voltage step manipulation protocols, which manipulated the membrane potential of a cell gradually by successive increments of 40 mV/500 ms voltage steps, inducing net voltage alterations ranging from -20 mV to +140 mV over the course of ~22 seconds. The PackIO recordings were coupled with fluorescent voltage imaging recordings that were performed under 642 nm 'Arch laser' (Coherent: OBIS) excitation.

E. Data Processing

As a preliminary check, we used ImageJ (NIH) to process fluorescence recordings and derive Fluorescence vs. slices (equivalent to time) plots. All subsequent data were derived via MatLab (Mathworks).

III. RESULTS

A. Criteria for Data Selection

In analysis, we selectively excluded data that were problematic in one or more respects. Foremost, neurons with aspiny dendrites, in other words dendrites with little to no dendritic spines, provided no data to work with. Neurons that did possess spiny dendrites when viewed at 1 binning/300 msec exposure time but were too dim to show any spines to select during 4 binning/10 msec exposure time voltage imaging either due to progressive photo-bleaching, low baseline voltage indicator expression and fluorescence, or excessive background fluorescence due to high cell density were also excluded. Finally, a number of cells, particularly during 20 msec current injection protocols, exhibited spontaneous firing even without stimulation; this disrupted the MatLab program's capability to synchronize the electrophysiology recordings with voltage imaging recordings. Many 20msec- pulse protocol recordings were excluded due to this phenomenon. Though some of these omissions are contingent on technical limitations of our methods and may cause us to overlook some potentially viable data, we believe such overall necessarily excludes confounds and noise from our final results

at the cost of a smaller sample size.

B. ArcLight: Current Injection and Shaft-Spine Voltage Imaging for Exemplary 'Cell A'

We present the data from current injections and voltage imaging of a single representative shaft-spine pair from 'Cell A'. Under bright-field microscopy at 60x magnification, cell A exhibits normal neuronal morphology very faintly, partially due to overpopulation and high cell density of the culture (**Fig. 1A**). Cell A as identified via epifluorescence microscopy of GFP under 570nm excitation (included in ArcLight; no additional marker was used) indicates very spiny dendrites, as well as appropriate localization of the genetically encoded ArcLight to the plasma membrane and dendritic spines (**Fig. 1B**).

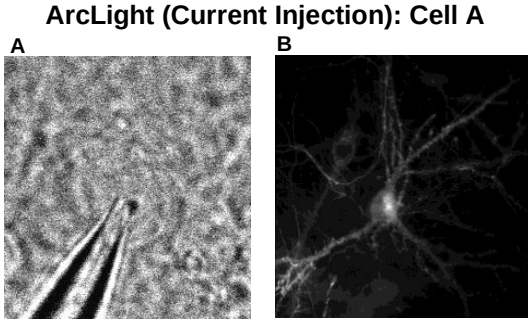

Figure 1. ArcLight: 'Cell A'
A. Cell A as seen by bright-field microscopy under 60x magnification, with micropipette visible. **B.** Cell A as seen by epifluorescence microscopy of the GFP contained in ArcLight (no additional reporter was required).

Cell A was whole-cell patch clamped and subjected to a current injection protocol that applied a total of 10 pulses, each of 250 pA magnitude and 100 ms duration, over the duration of ~12 seconds; neuronal membrane potential responses to 9 of the pulses are selected here for ideal visualization (**Fig. 2**). For a selected region of interest (ROI) (**Fig. 2A**) indicating either a given dendritic shaft or its adjacent spine, we synchronized whole cell membrane potential recordings with local fluctuations in fluorescence and plotted both voltage and ΔF/F with respect to time for the duration of the simultaneous recordings. Fluorescence changes (blue) coincide only very weakly with peak voltage fluctuations (green), presumably due to the low relative signal-to-noise of ArcLight (**Fig. 2B**).

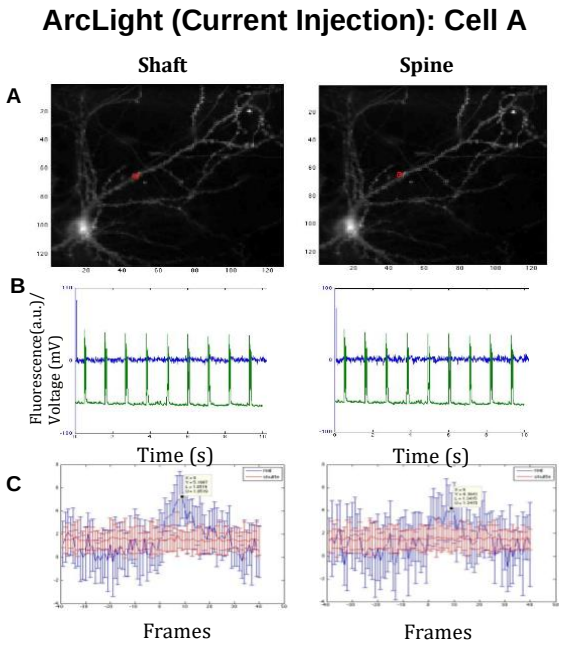

Figure 2. ArcLight: Current Injection Electrophysiology and ΔF/F of Dendritic Shaft vs. Spine in 'Cell A'
A. The region of interest (ROI) for ΔF/F comparison in a single dendritic shaft-spine pair for Cell A, indicated by the red boundaries as selected during data processing and analysis. **B.** Whole cell electrophysiological recordings of voltage (green) and local fluctuations in ΔF/F (blue) in a single recording session of the aforementioned shaft-spine pair, synchronized on a time axis. **C.** Spike-triggered average (STA) for the aforementioned shaft-spine pair. This represents the average ΔF/F (blue) of a specific ROI, in response to each and every induced bAP within a given train of current injections. The peak after frame=0 that spikes above the baseline fluorescence (red) was selected as the peak ΔF/F to be used in shaft vs. spine comparison.

Spike-triggered average (STA) data

presents an averaged representative ΔF/F response to one induced bAP for the selected ROI, based on voltage-fluorescence synchro-nizations; the data given indicates a ~5% peak change in fluorescence for a ROI of the shaft and a ~4% peak change in fluorescence for its adjacent spine (**Fig. 2C**).

C. ArcLight: Mean Peak ΔF/F of Shaft vs. Spine

From the STA data (exemplified in **Fig. 2C**) of multiple imaged shaft-spine pairs, we summed the peak ΔF/F of all shaft ROIs and of all spine ROIs, and compared the mean peak ΔF/F of the dendrite shaft (blue) to the mean peak ΔF/F of its adjacent spine (red) for long pulse (100 ms) and short pulse (20 ms) current injection protocols respectively (**Fig. 3**). Taking standard deviation into account, neither the long pulse nor the short pulse current injection/ voltage imaging results indicate a statistically significant dampening of peak ΔF/F from the dendrite shaft to its adjacent spine. However, the data does seem to suggest a potential difference in ΔF/F change between the long pulse and short pulse current injections, in that the 100 ms pulse injection protocol seems to potentially show greater dampening of ΔF/F in the spine, relative to the negligible ΔF/F difference in shaft to spine of the 20 ms protocol (**Fig. 3A, B**).

D. Arch: Current Injection and Soma Voltage Imaging for Exemplary 'Cell B1' and 'Cell B2'

As with ArcLight, we present the data from current injections and voltage imaging of representative neurons 'Cell B1' and 'Cell B2', respectively expressing the QuasAr1 and QuasAr2 variants of Arch. Under bright-field microscopy at 60x magnification, both Cell B1 and Cell B2 show normal, healthy neuronal morph-ologies (**Fig. 4A**) in particular comparison to ArcLight-expressing Cell A (**Fig. 1A**). Epifluorescence microscopy using the co-expressed mOrange reporter protein indicates sufficient expression for both cells, albeit relatively scarce dendritic spine distributions (**Fig. 4B**). Illumination under an Arch-specific laser (642 nm) at 110 mW output indicates intense expression of the respective Arch variants for each cell (**Fig. 4C**).

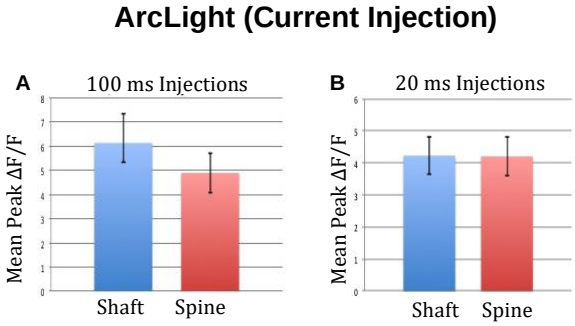

Figure 3. ArcLight: Mean Peak ΔF/F of Shaft vs. Spine for Long Pulse (100msec) and Short Pulse (20msec) Current Injection Recordings
A. The mean peak ΔF/F STA with standard deviation (%) of shaft vs. spine in ArcLight voltage imaging of a total of 21 shaft-spine pairs, for the long pulse (100msec) current injection protocol. **B.** The mean ΔF/F STA with standard deviation (%) of shaft vs. spine in ArcLight voltage imaging of a total of 6 shaft-spine pairs, for the short pulse (20msec) current injection protocol.

Cell B1 and B2 were whole-cell patch clamped and both subjected to the same current injection protocol, which injected a total of 30 pulses, each 200 ms, over a duration of ~33 seconds. Instead of a shaft-spine pair, an ROI of the soma illuminated by the Arch laser was selected for analysis for both cells as a test of efficacy (**Fig. 5A**). Both cells responded to their respective current injections by firing a train of action potentials in response to each pulse (**Fig. 5B**). Voltage recordings corresponding to all 30 pulses for each cell were synchronized with fluorescence on a time axis; results do not visibly resolve individual fluorescence spikes (**Fig. 5C**). The STAs for both

QuasAr1 in Cell B1 and QuasAr2 in Cell B2 show negligible signal relative to background fluorescence, presumably due to excessively high laser output and/or excessive noise (**Fig. 5D**).

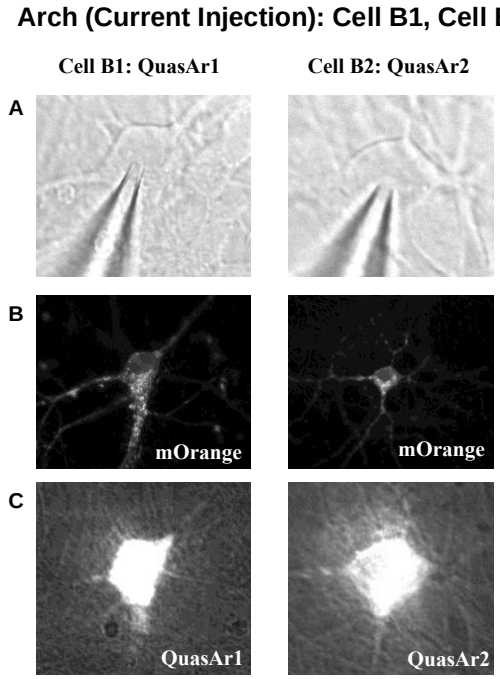

Figure 4. Arch: 'Cell B1', 'Cell B2'
A. Cell B1 (left) and Cell B2 (right) as seen by bright-field microscopy under 60x magnification, with micropipettes visible. **B.** Cell B1 (left) and Cell B2 (right) expressing an mOrange reporter protein, as seen by epifluorescence microscopy. **C.** Cell B1 (left) and Cell B2 (right) expressing QuasAr1 and QuasAr2 respectively, as seen by epifluorescence microscopy coupled with 642nm Arch laser illumination (110 mW).

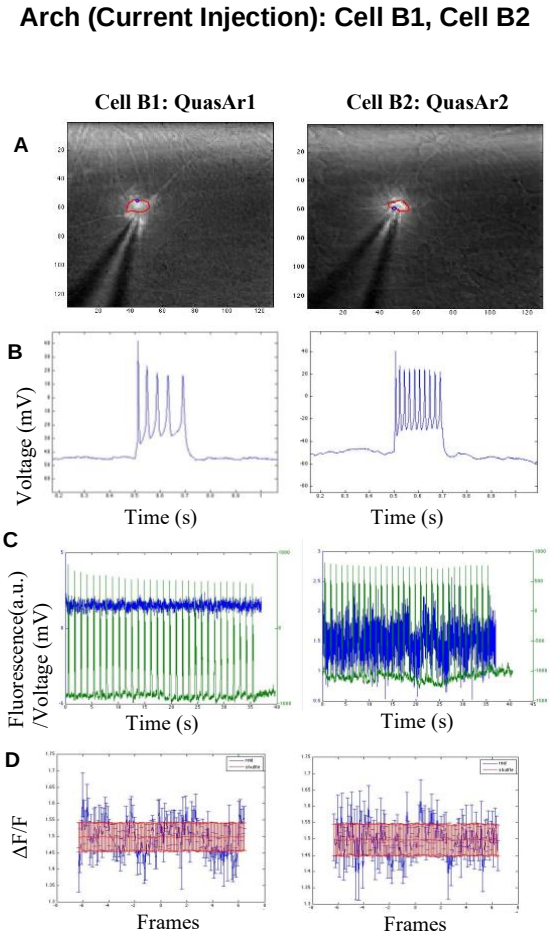

Figure 5. Arch: Current Injection Electrophysiology and ΔF/F of Soma in 'Cell B1' and 'Cell B2'
A. The region of interest (ROI) for ΔF/F in soma for Cell B1 (left) and Cell B2 (right), indicated by the red boundaries. **B.** Membrane potential fluctuations in Cell B1 (left) and Cell B2 (right) **i**n response to a single long current pulse (200msec) injection. **C.** Whole cell electrophysiological recordings of voltage (green) and local fluctuations in ΔF/F (blue) in a single recording session of soma for Cell B1 (left) and Cell B2 (right), synchronized on a time axis. **D.** Spike-triggered average (STA) for Cell B1 (left) and Cell B2 (right). This represents the average ΔF/F of a specific ROI, in response to each and every induced bAP within a given train of current injections.

E. Arch: Voltage Step Manipulation and Soma Voltage Imaging for Exemplary 'Cell C'

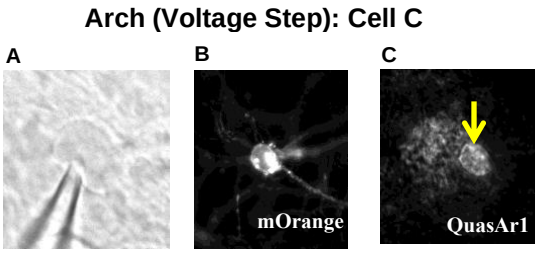

Figure 6. Arch: 'Cell C'
A. Cell C as seen by bright-field microscopy under 60x magnification, with micropipettes visible. **B.** Cell C expressing an mOrange reporter protein, as seen by epifluorescence microscopy. **C.** Cell C expressing QuasAr1 (yellow arrow), as seen by epifluorescence microscopy coupled with 642nm Arch laser illumination (10 mW)

To correct for the negligible signal given in **Figure 5D**, we performed direct, large-scale voltage step manipulations of membrane potential and simultaneous QuasAr1 voltage imaging in exemplary 'Cell C'. Cell C shows normal, healthy neuronal morphology under 60x bright-field microscopy (**Fig. 6A**) as well as epifluorescence microscopy visualizing the mOrange reporter (**Fig. 6B**). For QuasAr1 fluorescence, the Arch laser output was decreased drastically from 110 mW to 10mW, and brightfield microscopy was temporarily turned off to eliminate noise; Cell C is shown expressing QuasAr1 towards the peripheries of the range of laser-illumination (**Fig. 6C**).

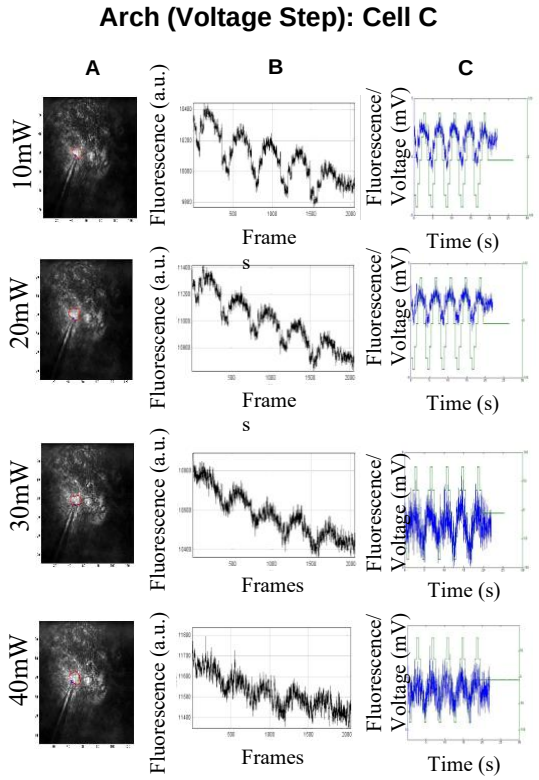

Figure 7. Arch: Voltage Step Electrophysiology and ΔF/F of Soma in 'Cell C'
A. Four distinct ROIs of Cell C soma, selected in 4 different QuasAr1 voltage step manipulation and voltage imaging recordings using 4 different respective laser intensities (10mW, 20mW, 30mW, and 40mW). **B.** General fluorescence fluctuations of QuasAr1 in response to voltage step manipulations, as seen in Cell C soma imaging using 4 different respective laser intensities. **C.** Whole cell electrophysiological recordings of voltage (green) and local fluctuations in ΔF/F (blue) in a single recording session of soma for Cell C, synchronized on a time axis.

We applied a voltage step protocol that manipulated the membrane potential of Cell C by 40 mV/500 ms voltage step increments, for a net alteration ranging from -20 mV to +140 mV over a duration of ~22 seconds. Four successive recordings were performed on Cell C at laser outputs of 10 mW, 20 mW, 30 mW and 40 mW, and similar ROIs were selected from all four recordings for analysis and comparison (**Fig. 7A**). Preliminary ΔF vs. time plots of image stacks derived from voltage imaging recordings indicate the largest QuasAr1 signal at 10 mW laser output, with fluorescence fluctuations corresponding to individual voltage steps visible; subsequently higher intensities of laser output seem to generate excessive noise relative to Arch signals, and the fluorescence 'steps' are rendered increasingly less visible towards 40 mW output (**Fig. 7B**). Fluorescence fluctuations

corrected for bleaching and synchronized with membrane potential fluctuation recordings on a time plot further demonstrate this trend; the characteristic parabola of ΔF as corresponding to the shape of the voltage waveform is rendered unrecognizable starting at 30 mW laser intensity (**Fig. 7C**).

IV. DISCUSSION

We hypothesized a dampening of membrane potential from the dendritic shaft into its adjacent dendritic spine as a test of the theory of spine electrophysiological compartmentalization. ArcLight voltage imaging of induced bAPs in mouse hippocampal neurons does not in fact seem to indicate a statistically significant dampening of membrane potential in the spine relative to the dendrite shaft. There does, however, seem to be some suggestion of a difference in membrane potential alteration at the spine between electrophysiological dynamics induced by long (100 ms) and short (20 ms) current injections, in other words between a train of multiple bAPs in rapid succession vs. single bAPs (**Fig. 3**).

Considering the nature of bAPs as primarily passively transmitted potentials, one would expect some amount of default deterioration as a bAP progresses across a dendrite into a spine. However, results from this study's ArcLight voltage imaging indicate not only that there is no immediately significant default deterioration (i.e., dampening) of potential, but also that a more prolonged stimulus (~100 ms current injection) inducing multiple bAPs may entail greater dampening than that caused by a small stimulus (~20 ms current injection) inducing a single bAP. This seems to contradict any initial assumptions that a passively traveling membrane potential would be prevented from deteriorating, i.e. dampening, if it is 'reinforced' by multiple subsequent bAPs. Rather, assuming our ArcLight imaging results are valid, our study may indicate that, in dendritic spines, weaker bAPs tend to be conserved while stronger, 'reinforced' bAPs are likely to be dampened, possibly in association with and/or manifested as phenomena such as long-term potentiation.

Caution must be taken, however, concerning the sheer number of possible neuronal subtypes and the consequent variability in neuron electrophysiology. Literature indicates that inhibitory GABAergic interneurons, and even SOM interneurons which comprise a subcategory of inhibitory interneurons, may be divided into a number of subtypes according to their electrophysiology[15, 16]. The indiscriminate nature of this study in terms of neuronal subtypes suggests that certain trends may very well have been overlooked or overemphasized.

We have thus started preparations for more precise imaging of spines, by optimizing two variants of Arch, QuasAr1 and QuasAr2, reported to be superior to ArcLight in fluorescence and kinetics under optimized conditions, in voltage imaging of neuronal soma. Our initial results from Arch with current injections, as had been done with ArcLight, indicated nearly negligible signal-to-noise ratios for both variants (**Fig. 5D**). Subsequent voltage imaging of voltage step manipulations with QuasAr1, performed at reduced brightfield noise and lower laser intensities (~10 mW vs. the previous ~110 mW), indicates that, to utilize the sensitivity of Arch in capturing spine electrophysiology, voltage imaging must be performed at reasonably low laser intensities (~10 mW) to prevent saturation.

Depending on further investigation of spine electrophysiology at a higher spatio-temporal resolution, it may be possible to more robustly demonstrate that dendritic spines discriminate between weak and strong stimuli. In conjunction with the results we have attained so far via ArcLight,

this would lend support to the hypothesis arguing for the electrophysiological compartmentalization and specialization of dendritic spines; elucidation of a component crucial in the composition of larger-scale neuronal circuits and patterns.

V. References

[1] Alivisatos, A., Chun, M., Church, G., Greenspan, R., Roukes, M. and Yuste, R. (2012).

[2] The brain activity map project and the challenge of functional connectomics. *Neuron* **74**, 970-974.

[3] Yuste, R. (2011), Dendritic spines and distributed circuits. *Neuron* **71**, 772-781.

[4] Cash, S., and Yuste, R. (1999). Linear summation of excitatory inputs by CA1 pyramidal neurons. *Neuron* **22**, 383-394.

[5] Yuste, R., and Denk, W. (1995). Dendritic spines as basic functional units of neuronal integration. *Nature* **375**, 682-684.

[6] Koch, C., and Zador, A. (1993). The function of dendritic spines: devices subserving biochemical rather than electrical compartmentalization. *J. Neurosci.* **13**, 413-422.

[7] Holthoff, K., Zecevic, D., and Konnerth, A. (2010). Rapid time course of action potentials in spines and remote dendrites of mouse visual cortex neurons. *J. Physiol.* **7**, 1085- 1096.

[8] Koester, H.J., and Sakmann, B. (1998). Calcium dynamics in single spines during coincident pre- and postsynaptic activity depend on relative timing of back-propagating action potentials and subthreshold excitatory postsynaptic potentials. *Proc. Natl. Acad. Sci. USA* **95**, 9596-9601.

[9] Grienberger, C. and Konnerth, A. (2012). Imaging calcium in neurons. *Neuron* **73**, 862- 885.

[10] Peterka, D., Takahashi, H., and Yuste, R. (2011). Imaging voltage in neurons. *Neuron* **69**, 9-21.

[11] Jin, L., Han, Z., Platisa, J., Wooltorton, J., Cohen, L., and Pieribone, V. (2012). Single action potentials and subthreshold electrical events imaged in neurons with a fluorescent protein voltage probe. *Neuron* **75,** 779-785.

[12] Kralj, M. J., Douglass, A. D., Hochbaum, D. R., Maclaurin, D., and Cohen, A. (2012). Optical recording of action potentials in mammalian neurons using a microbial rhodopsin. *Nature Methods* **9:1**, 90-95.

[13] Maclaurin, D., Venkatachalam, V., Lee, H., and Cohen, A. (2013). Mechanism of voltage-sensitive fluorescence in a microbial rhodopsin. *PNAS* **110:15**, 5939-5944.

[14] Akemann, W., Mutoh, H., Perron, A., Rossier, J., and Knopfel, T. (2011). Imaging brain electric signals with genetically targeted voltage-sensitive fluorescent proteins. *Nature Methods* **7:8**, 643-649.

[15] Stuart, G., Spruston, N., Sakmann, B., and Hausser, M. (1997). Action potential initiation and backpropagation in neurons of the mammalian CNS. *TINS* **20:3**, 125-131.

[16] Ascoli, G. A., et al. [The Petilla Interneuron Nomenclature Group (PING)]. (2008). Petilla terminology: nomenclature of features of GABAergic interneurons of the cerebral cortex. *Nat Rev Neurosci.* **9:7**, 557-568. doi:10.1038/nrn2402.

[17] McGarry, L. M., Packer, A. M., Fino, E., Nikolenko, V., Sippy, T., and Yuste, R. (2010). Quantitative classification of somatostatin-positive neocortical interneurons identifies three interneuron subtypes. *Frontiers in Neural Circuits* **4:12**, 1-19.